Unified Analysis for Antenna Pointing and Structural Errors Part I. Review

K. Abichandani
Ground Antennas and Facilities Engineering Section

A necessary step in the design of a high-accuracy microwave antenna system is to establish the signal error budget due to structural, pointing, and environmental parameters. This report, the first of a series, deals with a unified approach in performing error budget analysis as applicable to ground-based microwave antennas of different size and operating frequency.

A discussion of major error sources contributing to the resultant deviation in antenna boresighting in pointing and tracking modes and the derivation of the governing equations are presented. Two computer programs (SAMCON and EBAP) have been developed in-house, including the antenna servo-control program, as valuable tools in the error budget determination. A list of possible errors giving their relative contributions and levels is presented.

I. Introduction

The primary mission of a microwave antenna system is to receive signals from a deep space target either by automatic tracking or by pointing at the target in response to a predetermined command pattern. Both the accuracy in pointing the microwave beam and the precise automatic tracking become imperative and require a careful investigation of the bounds of each (Refs. 1 to 14). As the antenna size and the communication frequency increase, the size of errors and the resulting gain loss take on additional importance.

The practice by microwave and structure engineers in designing new microwave antennas is readily available in the literature. Antennas of different size, operating frequency, and mount have been designed and constructed in the past in different countries. Their design specifications of the allowable deviations from a true theoretical behavior have been assumed based on past experience. Also, there has been a lack of sufficient theoretical background for error predictions based on a unified approach to quantify the errors prior to antenna construction.

This report attempts to bridge the gap by outlining, in a unified approach, methods to determine the contribution by various structural/pointing sources of error on the overall signal gain loss during antenna pointing and/or tracking

regardless of the antenna configuration, size, operating frequency, etc.

II. Analysis

Errors may be classified broadly into two principal categories: dependent errors and independent errors. Dependent errors may be grouped together to form independent sets. Examples of dependent error sources are errors due to wind on the main reflector, supports, feed cone intermediate reference assembly, and the instrument tower. Each independent set, and individually independent error sources, may be applied to appropriate input points of the system for evaluation. To clarify this point, Fig. 1 depicts the antenna control system block diagram for one axis movement of the antenna and indicates likely error sources. Their contribution to the total signal error naturally depends upon positioning. To illustrate this effect, let us consider the simplified representation depicted in Fig. 2 where G_1, G_2, and H are the Laplace transforms for a general closed-loop control system components that could represent an antenna control system. For example, R is the controlled quantity (e.g., antenna position in elevation angle, declination angle, or azimuth angle), C is the command signal, and E is the error between the command and generally modified (or shaped) controlled quantity R. If S_i ($i = 1, 2, 3$) are the error sources applied at the components G_1, G_2, and H, one may write, in general,

$$\frac{R}{C} = \frac{G_1 G_2}{1 + HG_1 G_2} \tag{1}$$

$$\frac{E}{C} = \frac{1}{1 + HG_1 G_2} \tag{2}$$

$$\frac{R}{S_1} = \frac{G_1 G_2}{1 + HG_1 G_2} \tag{3}$$

$$\frac{R}{S_2} = \frac{G_2}{1 + HG_1 G_2} \tag{4}$$

$$\frac{R}{S_3} = \frac{HG_1 G_2}{1 + HG_1 G_2} \tag{5}$$

Equations (1) through (5) are general for the control system shown and will be used in determining errors in antenna pointing and tracking.

III. Error Sources and Points of Application

Ten major error sources were identified and grouped as follows:

(1) Command errors.

(2) Command quantizing errors.

(3) Structure dead load errors.

(4) Wind-induced errors.

  (a) Steady wind errors.

  (b) Random wind effect.

  (c) Turbulent wind component.

(5) Data system errors.

(6) Tracking errors.

(7) Thermal errors.

(8) Structural tolerances and alignment errors.

(9) Servo control system errors.

(10) Refraction, microseism and instrument errors.

Each error source is discussed in detail as follows:

A. Command Errors

Commands are generally given according to predetermined positioning and rate schedule, e.g., a position command, or a tracking command. If an error is made in the predetermination of the commands, an error is naturally introduced at the outset. The error ΔC will be attenuated as follows: if ΔR is the change in the controlled quantity, then from Eq. (1),

$$\Delta R = \Delta C \frac{G_1 G_2}{1 + HG_1 G_2} \tag{6}$$

B. Command Quantizing Errors

In the case of an antenna tracking a space vehicle, the vehicle orbit is known a priori. By computation on a digital computer, the orbit configuration data are stored and the command signals are derived from this stored information in binary form. The quantizing error usually has a distribution of one bit. This amounts to 1 arcsecond rms in azimuth angle for a 20-bit quantization of the encoder.

C. Structure Dead Load Errors

Forces due to gravity resulting in moments on the structure deflect the members and panels, causing a change of shape of the antenna. As the elevation varies, so do the moments of

forces giving rise to structural deflections. However, the moments of forces are predictable (Refs. 8 to 14) and repeatable within the hysteresis characteristics of the structure. These characteristics can be determined a priori and stored by a computer program and thus calibrated out rather accurately. The compensation due to this effect will be discussed later in Section IV.

D. Wind-Induced Errors

The wind effect may be decomposed into two portions: first the portion due to a steady wind, second the portion due to a variable wind comprising gusts and direction changes. The two components of wind produce forces and moments on the antenna structure which can be superimposed and result in the boresight errors. Each portion is discussed below.

1. Steady wind errors. Steady wind may be analyzed by considering the aerodynamics of its flow on structures. The laminar or low Reynolds number component causes drag and lift forces that cause steady moments, depending on the location of the center of pressure.

The steady wind also has turbulent component and vortices associated with it. Turbulent flow results in high frequency variations, which the inertia of the antenna structure filters out. Vortex flow results in low frequency variations that require further consideration. These variations are amenable to power density analysis. If the "pure" steady-state wind velocity is V, the associated moment M may be computed as

$$M = \frac{\rho}{2} V^2 S \bar{c} C_m \tag{7}$$

where

ρ = density of air at sea level

V = wind velocity

S = projected area of the antenna dish

C_m = moment coefficient

$\bar{c}$ = mean diameter of the antenna

Once C_m is established, the moment can be computed. Knowing the stiffness of the structure, the deflection can be determined. The effect of "purely" steady wind from Eq. (7) can consequently be compared to that due to the gravity loading discussed above.

The effects of wind-induced stresses on the antenna structure have been addressed in detail in Ref. 8.

2. Random wind effect. In order to evaluate the effect of the random wind on the antenna structure (input) we will use the method which determines the mean square error in the antenna rigid body dynamics (output) resulting from a finite torque power spectrum. Let the power spectral density (PSD) of the variable wind distribution be denoted by $S_w(jw)$, and the general linear system transfer function of the antenna by $Y(jw)$; the mean square error $\overline{\theta}^2$ of the controlled quantity may be expressed as (Ref. 15)

$$\overline{\theta}^2 = \int_{-\infty}^{\infty} |Y(jw)|^2 S_w(jw)\, dw \tag{8}$$

where $Y(jw)$ is a general term representing either the dynamics of the antenna control system or the flexible dynamics of the antenna structure. The antenna servo-control simulation program, SAMCON, initiated by Ref. 16 performs, among others, the operation represented by Eq. (8) for the computation of the random wind effects.

3. Turbulent wind component. The power spectral density of the wind acting on the supporting structure is not largely different from that acting on the antenna main reflector. The only difference will be in the magnitude of the PSD of the torque due to the wind. The transfer function $Y(jw)$ associated with the supporting structure will have a form similar to that for the antenna dynamics, i.e., a second-order system transfer function represented by the following expression:

$$Y(jw) = \left(\frac{a_2 S^2 + a_1 S + a_0}{S^2 + 2\zeta W_n S + W_n^2} \right)_{s = jw} \tag{9}$$

where a_0, a_1 and a_2 are constants, ζ is the structural damping ratio, and W_n is the structural natural frequency of the mode selected for the analysis. The selection criterion considers the bandwidth of the antenna servo-control loop in the case of the antenna. In the case of the supporting structure, its modal frequencies within or near the wind spectrum may be examined.

The following widely accepted expression derived in Ref. (17) may be used for the wind PSD used in Eq. (8).

$$S_w(jw) = \frac{K_w}{(w_0^2 + w^2)(w_1^2 + w^2)} \tag{10}$$

where

S_w = wind torque PSD

K_w = constant establishing torque level which is written as

$$K_w = 4\alpha^2 w_0 w_1 (w_0 + w_1) T_0^2/\pi \qquad (11)$$

where

α = rms turbulence wind speed variation about the mean wind speed T_0: typically = 0.2

w = frequency in radians/sec

w_0 = frequency at first "break corner," radians/sec

E. Data Encoding/Displaying System Errors

If the antenna position and rate are remotely monitored in a central control room, the fine instruments, measuring that antenna position or rate including pinions, encoders, display, etc., may indicate erroneous readings due to errors inherent in the measuring instrument itself. One way to determine such errors is by statistically determined test data over a certain period of time. Sample values of typical error sources in antenna components are presented in Table 1 for information.

F. Track Errors

Tracking error can be defined as the space angle difference between the communication RF axis of the antenna and the vector to the RF source being tracked. The servo-control simulation program, SAMCON, which is being developed inhouse, provides the tracking error magnitude. One may choose arbitrarily the pickoff point for the position feedback which affects antenna structural flexure influence on the tracking errors. If data system gears are used, then the flexure effects will be circumvented. Additional details about the inputs and outputs for this program will be addressed in detail in a separate publication.

G. Thermal Errors

Another major source of error is that due to the temperature gradient in the various members of the antenna structure. Although the effect of the temperature gradient on an individual member can be predicted and accurately determined, determination of the combined effect of all the members comprising the antenna structure is a complex task. One approach would be to develop a computerized thermal model to determine the deformations and the resultant antenna errors. However, in the absence of such a model at present, field data from existing antennas may be used (Ref. 18). The main source of thermal error may be assumed to be due to the supporting structure, e.g., quadripods and the reflector supports. A pattern of temperature gradient from this data may be assumed; however, this procedure is approximate. Sometimes the thermal effects may be accounted for by using an empirical correction factor > 1.0 to be applied to the errors computed due to the dead load. The development of a good thermal model is now in progress (Ref. 19) to satisfy this need.

H. Structural Tolerances and Alignment Errors

This alignment error category may be divided into five major areas comprising:

(1) Alignment of radio frequency boresight axis to an Intermediate Assembly (IRA) (wherever existing).

(2) Alignment of an IRA to elevation axis, if IRA is provided.

(3) Alignment of elevation axis to azimuth axis.

(4) Alignment of azimuth axis to earth reference system.

(5) Runout of azimuth and elevation drive bearings.

The alignment of the RF boresight axis to an IRA is the most crucial one. The error consists of field alignment of the hyperboloid subreflector and its supports, field setting and alignment of the paraboloidal reflector and its supports including face panels, field alignment of the feed cone, and field alignment of the IRA. Contributions from the individual sources to the total boresight shift make up one large error which is part of the RF boresighting problem to be addressed later.

The RF boresighting problem involves the method of making the pattern measurement and boresighting the RF axis to the mechanical axis represented by the IRA. This problem consists of accurately locating a source of RF energy which can be moved throughout the hemisphere of coverage at ranges great enough to include the atmospheric refraction of the RF energy. Several methods have been considered for obtaining the location of the boresight axis relative to some reference point in space. The method with good promise is to arrive at the boresight error by CONSCAN techniques of pointing on a radio star (Ref. 20). However, this error can be determined rather accurately and corrected for by properly aligning the structure from the RF boresight to the IRA; the design of the data system eliminates the remaining structural manufacturing and alignment errors from the system output. The four errors that can thus be eliminated include (1) alignment of the IRA to elevation axis, (2) alignment of elevation to the azimuth axis, (3) alignment of the azimuth axis to an earth reference system, and (4) bearing runout.

The total effect of the above errors (derived in Ref. 21) is given in the Appendix and results in the following two equations.

$$
\begin{aligned}
Error\,(C)_x = & -S_1 + C_1\,[\cos(h - C_2)]\left(\frac{\partial X}{\partial h}\right)_\psi - S_2 \tan Y \sin X \\
& + S_3 \tan Y \cos X - S_4 \tan Y + \frac{C_3}{\cos Y} \pm S_5 \\
& + A_3 \ddot{X} - S_7 \left(\frac{\partial X}{\partial \lambda}\right)_\phi + A_2 \frac{X}{|X|} + A_5 \frac{\dot{X}}{|\dot{X}|} \\
& + S_8 \left(\frac{\partial X}{\partial \phi}\right)_\lambda + A_7 \dot{X} + A_9 \frac{\sin 2\theta}{\cos Y} \qquad (12)
\end{aligned}
$$

$$
\begin{aligned}
Error\,(C)_y = & \; C_6 + C_4\,[\cos(h - C_5)]\left(\frac{\partial Y}{\partial h}\right)_\psi - S_2 \cos X \\
& - S_3 \sin X \pm S_6 + A_1 \ddot{Y} - S_7 \left(\frac{\partial Y}{\partial \lambda}\right)_\phi \\
& + A_4 \frac{Y}{|Y|} + A_6 \frac{\dot{Y}}{|\dot{Y}|} + S_8 \left(\frac{\partial Y}{\partial \phi}\right)_\lambda + A_8 \dot{Y} \\
& + A_{10} \sin 2\theta + A_{11} \cos 2\theta \qquad (13)
\end{aligned}
$$

where (X, Y) is generalized position coordinates, $(\dot{X}, \dot{Y})$ is the velocity, $(\ddot{X}, \ddot{Y})$ is the acceleration, A and C are coefficients to be determined by field measurements, and S's are biases. Although the equations were originally derived for a 9-meter antenna operating in the S-band frequency (Ref. 21), their form and the technique used for evaluating the coefficients make them suitable without significant modifications for any size antenna system at any frequency. This is simply due to the fact that in the derivation followed there are no size- or frequency-dependent terms involved.

Equations (12) and (13) are algebraic summations of systematic RF to optical boresight error and optical boresight to true encoder axis error. The parameters X, Y, A, C, and S are listed in the definition of symbols table. Although the derivation of error equations was made with respect to two orthogonal axes, X and Y axes of the antenna, the analysis is still in general form and could be used for any two orthogonal coordinates. The only conditions to be satisfied are that (1) the axes be orthogonal, and (2) the chosen antenna axes relationship with these two orthogonal axes must be known a priori.

The five error sources that are included in the derivation of Eqs. (12) and (13) are

(1) X-Y antenna angular errors due to tilt of the primary (X) axis.

(2) X-Y antenna angular errors due to lack of orthogonality.

(3) Pointing error due to positioning errors in station location such as latitude and longitude of the antenna position.

(4) Pointing errors due to structural deflection.

(5) Boresight shift with polarization rotation.

The polarization rotation concerns unified S-band antennas and aircraft which were used to draw tracks providing linearly polarized transmission signals for measuring this error source (applicable to 9- to 26-meter antennas, Ref. 21). This error source is not applicable to nonpolarized signal transmission.

Equations (12) and (13) were programmed in-house in the Error Budget Analysis program (EBAP). In order to be able to determine the errors $(C)_x$ and $(C)_y$, all the coefficients in Eqs. (12) and (13) must be known a priori.

I. Servo Control System Errors

The error sources contributing to the positioning error of the antenna are:

(1) The type of the control system.

(2) Hardware.

(3) Tachometer.

The type of control system could be either type-1 or type-2. The error will be governed by the type of command to the particular type of system. For a type-2 system, a constant command will result in zero error; so will a constant rate command. Second, hardware such as motors, amplifiers, modulators, demodulators, synchros, etc., may have dead zones, thresholds, and tooth ripples which result in nonlinear operation near the theoretical zero error zones, such as final commanded position. Third, the function of the tachometer is to augment damping in a rate loop. Inaccuracy in the scale factor, presence of noise, and ripple will introduce error not only in following the rate commands, but also in the desired position because of effective nonlinear damping. Knowing the system dynamic characteristics from manufacturer's data, the servo simulation program (SAMCON), Ref. 16, provides the error magnitudes due to this source. Thus, all the errors in the control system may be determined.

J. Refraction, Microseism and Instrument Tower Errors

These sources of error have been reported to be insignificant. However, they are mentioned here briefly.

Refraction is an integral part of the boresight procedure which has been discussed earlier in Section III-H.

Microseisms, in general, consist of small amplitude, relatively high-frequency earth tremors. Microseisms can introduce errors into the system by disturbing the instrument tower. Reference 22 concluded that the largest error on the instrument tower caused by all possible sources was due to 96 km/hr (60 mph) wind blowing on the main reflector and transmitting overturning forces from the main pedestal through the earth to the instrument tower. This wind-induced error swamped out any errors due to microseisms. The magnitude of this error was about 0.3 arcseconds peak. Hence, microseisms are negligible compared to other errors in the system.

Having discussed the various error sources and the derivation of formulas to compute these, a list is given in Table 1 with some sample values.

IV. Relevant Work

In addition to the above pointing and tracking errors determination, other in-house work was initiated for determination of errors due to any reflector shape change, the consequent shift in the focal point of the main reflector, and the feed system components for a Cassegrain antenna. The pointing error sources were as follows (Ref. 23):

(1) Antenna primary reflector parabola translation.

(2) Primary reflector parabola rotation.

(3) Subreflector hyperbola translation.

(4) Hyperbola rotation.

Effect of wind load was included by applying a correction factor. This correction factor is the square of the ratio of two values of wind velocity: (1) the wind velocity for which the parameters are known a priori, and (2) the wind velocity for which the errors are to be computed.

The pointing error is computed as the root sum square (rss) of errors about two orthogonal axes in seconds of arc. This error source is root-sum-squared with the other sources discussed earlier. Changes in the shape of the antenna due to its dead weight and wind must be accounted for if errors are to be computed accurately.

V. Conclusions

Two computer programs (SAMCON and EBAP) were developed as analytical tools to support the error analysis study. Error equations for the EBAP program are listed in the Appendix. These programs will enable one to compute an error budget covering most of the sources outlined above.

Two major error sources emerged as requiring further development: one is the contribution by structural dynamics excited by some control commands and noise at various points of the antenna servo control system; the other is that due to thermal gradient. The first requires expanding the control simulation program (SAMCON) while the thermal gradient effect will require additional experimentation and analytical development.

In evaluating the errors given by Eqs. (12) and (13), some coefficients will have to be determined. By using known data from currently existing designs, preliminary error values may be computed. Updating the information after constructing any antenna will provide a better baseline for error determination of new ones. This is an iterative process which is important for designing new antennas in the future.

Acknowledgement

The author is indebted to R. Levy, M. Katow, H. Phillips, F. Lansing and I. Khan of the JPL Technical Staff for sharing their technical views and their editing contributions throughout this work.

References

1. Ruze, J., "Lateral Feed Displacement in a Paraboloid," *IEEE Trans. Ant. Prop.*, Sept. 1965, pp. 660-665, 1965.

2. Mar, J. W., and Liebowitz, J., Editors, *Structures Technology for Large Radio and Radar Telescope Systems*, The MIT Press, Massachusetts Institute of Technology, Cambridge, Mass., 1969, pp. 1-54.

3. Ibid, pp. 65-87.

4. Ibid, pp. 101-134.

5. Ibid, pp. 185-200.

6. Ibid, pp. 499-514.

7. Katow, M. S., Bartos, K. P., and Matsumoto, L. R., *JPL Modified STAIR Systems Operating Procedures*, NASA TM 33-304, Jet Propulsion Laboratory, Pasadena, Calif., June 1, 1968.

8. Levy, R., and Katow, M. S., "Implementation of Wind Performance Studies for Large Antenna Structures," *IEEE Mechanical Engineering in Radar*, pp. 27-33.

9. Levy, R., and Parzynski, W., "Optimality Criteria Solution Strategies in Multiple Constraint Design Optimization," 22nd Structures, Structural Dynamics and Materials Conference, Atlanta, Georgia, Apr. 6, 1981.

10. Levy, R., "Optimality Criteria Design and Stress Constraint Processing," Preprint, International Symposium on Optimum Structural Design, University of Arizona, Tucson, Oct. 19, 1981.

11. Katow, M. S., "Structural Design of a 64-Meter Low Cost Antenna," *DSN Progress Report 42-45*, Jet Propulsion Laboratory, Pasadena, Calif., pp. 258-275, June 15, 1978.

12. Levy, R., *Iterative Design of Antenna Structures*, Technical Report 32-1526, Vol. XII, Jet Propulsion Laboratory, Pasadena, Calif., pp. 100-111, Dec. 15, 1972.

13. Levy, R., "Conceptual Studies for New Low Cost 64-m Antennas," *DSN Progress Report 42-33*, Jet Propulsion Laboratory, Pasadena, Calif., pp. 55-67, June 15, 1976.

14. Katow, M. S., and Patton, R. H., "Structural Data Checks with Computer Graphics," *DSN Progress Report 42-27*, Jet Propulsion Laboratory, Pasadena, Calif., pp. 148-153, June 15, 1975.

15. Davenport, W. B., Jr., and Root, W. L., *An Introduction to the Theory of Random Signals and Noise*, McGraw-Hill Book Company, Inc., N.Y., 1958.

16. James, M. R., "The Implementation and Analysis of a Baseline Antenna Servo Control System Model," Report by Harris Corporation, Melbourne, Florida, for Jet Propulsion Laboratory, NASA Contract No. NAS7-100, Subcontract No. 956125, Apr. 1982.

17. Sweo, E. A., "Method of Calculation for Reflector Assembly Pointing Error," Dalmo Victor Co., Report DV-230-1B, Belmont, Calif., Oct. 1963.

18. Glazer, S., and Gale, G., "Thermal Measurement Technique of Rib Elements on DSN Antenna Structure," *TDA Progress Report 42-66*, Jet Propulsion Laboratory, Pasadena, Calif., pp. 67-79, Dec. 15, 1981.

19. Schonfeld, D., and Lansing, F., "Thermal Analysis of Antenna Backup Structure, Part I – Methodology Development," *TDA Progress Report 42-70*, Jet Propulsion Laboratory, Pasadena, Calif., pp. 110-116, Aug. 15, 1982.

20. Abichandani, K. P., and Ohlson, J. E., "Boresighting Techniques for the Antenna Control Assembly (ACA)," *TDA Progress Report 42-64*, Jet Propulsion Laboratory, Pasadena, Calif., Aug. 15, 1981.

21. Collins Radio Company, "Apollo Unified S-Band GSFC 30-Foot Antenna System, Kennedy Station," Engineering Report No. 1523=0559008-001 D3m, prepared for NASA Goddard Space Flight Center, Greenbelt, Md., Oct. 1966.

22. Isber, A. M., "Obtaining Beam-Pointing Accuracy with Cassegrain Antennas," *Microwaves*, pp. 40-44, Aug. 1967.

Definition of Symbols

A_1 Y acceleration error coefficient

A_2 X zenith structure shift

A_3 X acceleration error coefficient

A_4 Y zenith structure shift

A_5 X direction effect

A_6 Y direction effect

A_7 X velocity error coefficient

A_8 Y velocity error coefficient

A_9 X polarization shift component

A_{10} Y polarization shift component

A_{11} Y polarization shift component

C_1 X deflection coefficient in an elevation plane

C_2 X deflection angular offset in an elevation plane

C_3 Rf axis to Y axis lack of orthogonality (a positive sign means $|C_7|$ is subtracted from 90°) $\equiv \delta R$

C_4 Y deflection coefficient in an elevation plane

C_5 Y deflection angular offset in an elevation plane

C_6 RF axis to Y encoder axis bias

h elevation angle

S_1 X encoder bias

S_2 tilt component δV of the X axis, taken from a reference direction

S_3 tilt component δE of the X axis

S_4 X axis to Y axis lack of orthogonality (a positive sign means $|S|$ is subtracted from 90°) $\equiv \delta N$

S_5 X encoder hysteresis

S_6 Y encoder hysteresis

S_7 station longitude error ($\Delta\lambda$)

S_8 station latitude error ($\Delta\phi$)

t local hour angle

α, β, γ direction angles of target vector w.r.t. fixed frame

δ declination angle/infinitesimal change

θ the angle between a reference line on the antenna feed which is vertical when XY mount faces the east or south (depending on the antenna design) horizon and a constant vertical line.

λ station longitude angle

ϕ station latitude angle

ψ azimuth angle

Table 1. Sample values of some error sources

Type of error	Sample values (3σ) (for 64-m antenna), arcsec
Command error	
Input command determination	24
Input quantization	4
Command	7
Velocity	7
Acceleration	2
Friction	3
Tooth cogging and drive serve	15
Dead load errors	
Reflector	120
Hyperboloid translation	−14
Hyperboloid rotation	7
Intermediate reference assembly	21
Instrument mount	3
Wind-induced errors	
Steady wind (50 km/h)	5
Variable wind	25
Thermal errors	50
Structural tolerances and alignment errors	36
Data system errors	12
Alignment of normal to mirror surface parallel to normal to IRA	–
Optical path	
Alignment of 2-axis autocollimator to its support	–
Orthogonality between axes	–
Alignment of encoders	–
Encoder positional errors	–
Alignment of instrument mount to the gravity vector	–
Errors in digital computer and D/A converter	–
Errors in servo control system	–
Hardware	–
System type	–
Refraction, microseism	Less than 3

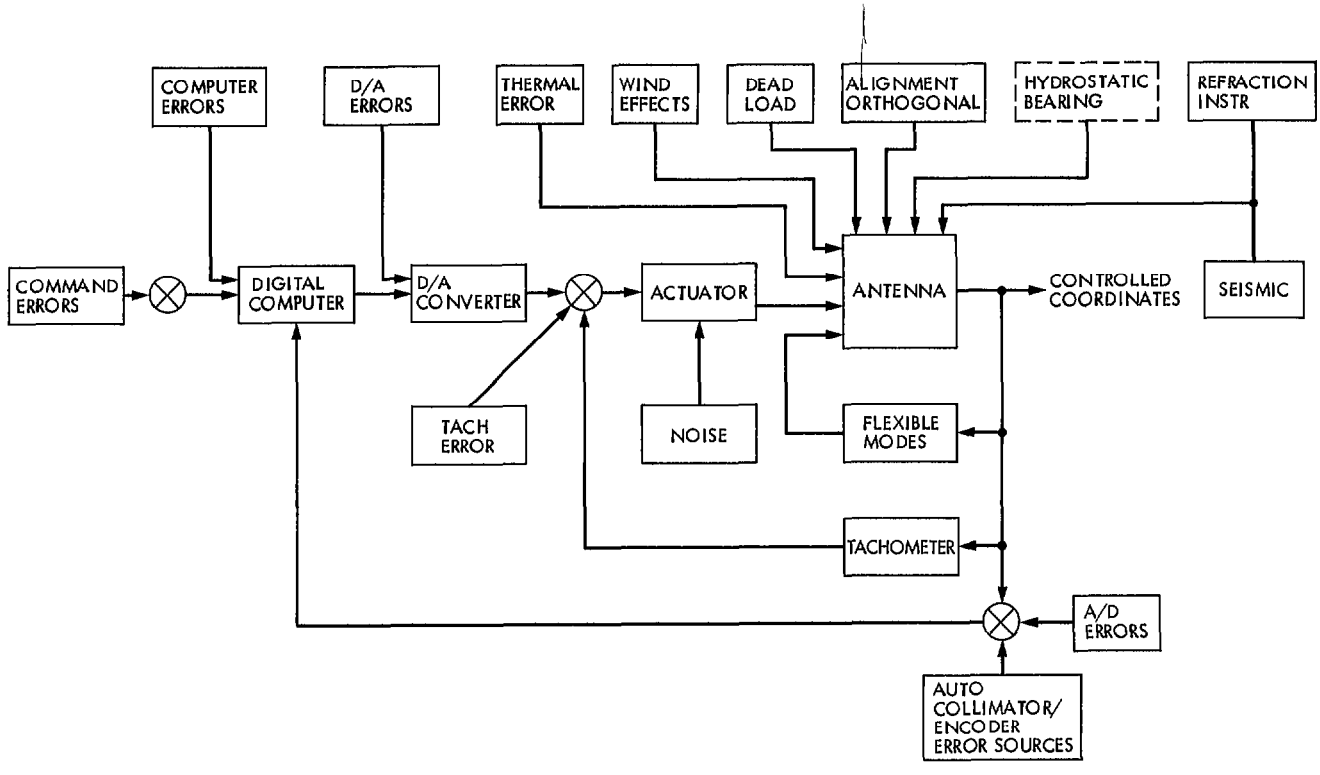

Fig. 1. Block diagram of error-source simulator

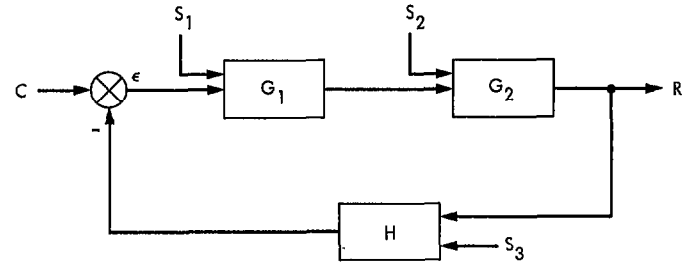

Fig. 2. Block diagram showing possible relative positions of error sources and control system components

Appendix

Error Equation Derivation

This appendix consists of derivations of several terms of the RF-to-encoder error equations. Spherical triangles are used since they display the error effects most vividly.

I. Antenna Angular Errors Due to Tilt of the Primary Axis

The two errors in X and Y angles, ΔX and ΔY, derived below[1], are those that occur as a result of successive rotation of the primary X axis of the antenna about each of the other two orthogonal axes. For small rotations, these are equivalent to two tilt components of the X axis. The following equations for ΔX and ΔY are used to solve for the axis misalignment or tilt components, δ_U and δ_E. The corrections, ΔX and ΔY, due to misalignment components δ_U, δ_E will be proved later as

$$\Delta X = \tan Y \, [\delta_U \sin X - \delta_E \cos X] \tag{A-1}$$

$$\Delta Y = \delta_E \sin X + \delta_U \cos X \tag{A-2}$$

where

$$\begin{aligned} X &= X' - \Delta X \\ Y &= Y' - \Delta Y \end{aligned} \tag{A-3}$$

In order to prove Eqs. (A-1) and (A-2) refer to Fig. A-1. The dotted tilted axes are obtained from the solid aligned axes (1), (2), and (3) by two steps:

(a) Rotate (2) by angle δ_U about axis (1) counterclockwise.

(b) Then rotate by angle δ_E about axis (3) clockwise.

Both components x, y, and z along axes (1), (2), and (3), and direction cosines cos α, cos β and cos γ of a target position vector have the same relations as follows, where primed values refer to tilted axes and unprimed values refer to aligned axes.

$$\begin{bmatrix} x' \\ y' \\ z' \end{bmatrix} = [BA] \begin{bmatrix} x \\ y \\ z \end{bmatrix}$$

and the new direction cosines are obtained from the unprimed direction cosines as

$$\begin{bmatrix} \cos\alpha' \\ \cos\beta' \\ \cos\gamma' \end{bmatrix} = [BA] \begin{bmatrix} \cos\alpha \\ \cos\beta \\ \cos\gamma \end{bmatrix} \tag{A-4}$$

where $[A]$ is the matrix obtained from step one and $[B]$ is the matrix obtained from step (b), above. $[BA]$ may be written as:

$$[BA] = \begin{bmatrix} \cos\delta_E & -\sin\delta_E & 0 \\ \sin\delta_E & \cos\delta_E & 0 \\ 0 & 0 & 1 \end{bmatrix} \begin{bmatrix} 1 & 0 & 0 \\ 0 & \cos\delta_u & \sin\delta_U \\ 0 & -\sin\delta_U & \cos\delta_U \end{bmatrix}$$

For small δ_E, δ_U, then, cos $\delta_E \to 1$, cos $\delta_U \to 1$, sin $\delta_U \to \delta_U$, sin $\delta_E \to \delta_E$, and $\delta_E \cdot \delta_U \to 0$, one may write $[BA]$ as[2]:

$$[BA] \cong \begin{bmatrix} 1 & -\delta_E & 0 \\ \delta_E & 1 & \delta_U \\ 0 & -\delta_U & 1 \end{bmatrix}$$

or

$$[BA] = \begin{bmatrix} 1 & 0 & 0 \\ 0 & 1 & 0 \\ 0 & 0 & 1 \end{bmatrix} + \begin{bmatrix} 0 & -\delta_E & 0 \\ \delta_E & 0 & \delta_U \\ 0 & -\delta_U & 0 \end{bmatrix} \tag{A-5}$$

[1] One must carefully distinguish between the angles (X, Y) and the moving two antenna axes (X, Y) and the space coordinates (x, y, z) for a target N under the reference axes (1), (2), and (3) in Fig. A-1.

[2] Equation (A-5) shows that $[AB] = [BA]$, which means that for small angles a reverse positioning of the axes will only reverse Eqs. (A-1) and (A-2).

Since the three direction cosines of the target position vector, ON, with respect to axes (1), (2) and (3), respectively are:

$$\cos\alpha = \cos Y \sin X \quad \text{(A-6a)}$$

$$\cos\beta = \sin Y \quad \text{(A-6b)}$$

$$\cos\gamma = \cos Y \cos X \quad \text{(A-6c)}$$

these may be used along with Eq. (A-5) in Eq. (A-4) to obtain three equations for $\cos\alpha'$, $\cos\beta'$ and $\cos\gamma'$ and solve for ΔX and ΔY as follows:

Using Eq. (A-6b) with Eq. (A-5) in Eq. (A-4) to obtain $\cos\beta'$ as

$$\sin Y' = \sin Y + \delta_E \cos Y \sin X + \delta_U \cos Y \cos X$$

Let

$$Y' = Y + \Delta Y$$

Hence,

$$\sin Y' = \sin Y \cos\Delta Y + \cos Y \sin\Delta Y$$

and for small ΔY

$$\sin Y + \cos Y \cdot \Delta Y = \sin Y + \delta_E \cos Y \sin X + \delta_U \cos Y \cos X$$

or

$$\Delta Y = \delta_E \sin X + \delta_U \cos X \quad \text{(A-7)}$$

Similarly from Eqs. (A-4), (A-5), and (A-6a), $\cos\alpha'$ is computed for small ΔX and ΔY,

$$(\cos Y - \sin Y' \cdot \Delta Y)$$

$$\times (\sin X + \cos X \cdot \Delta X) = \cos Y \sin X - \delta_E \sin Y$$

or

$$\cos Y \cos X \cdot \Delta X - \sin Y' \sin X \cdot \Delta Y = -\delta_E \sin Y \quad \text{(A-8)}$$

Also, from Eqs. (A-4), (A-5), and (A-6c), for small $(\Delta X, \Delta Y)$, $\cos\gamma'$ is written as

$$(\cos Y - \sin Y \cdot \Delta Y)$$

$$\times (\cos X - \sin X \cdot \Delta X) = \cos Y \cos X - \delta_U \sin Y$$

or

$$\cos Y \sin X \cdot \Delta X + \sin Y \cos X \cdot \Delta Y = \delta_U \sin Y \quad \text{(A-9)}$$

Multiplying Eq. (A-8) by $\cos X$, Eq. (A-9) by $\sin X$, adding and simplifying,

$$\Delta X = \tan Y \,[\delta_U \sin X - \delta_E \cos X] \quad \text{(A-10)}$$

Eq. (A-10) gives the correction ΔX in terms of δ_U and δ_E as shown in Eq. (A-1).

II. Antenna Angular Errors Due to Lack of Orthogonality

The two errors in X and Y angles, ΔX and ΔY, due to the lack of orthogonality of X, Y axes, δ_N, and between the positive RF and Y axes, δ_R, are derived. Both pairs of equations for ΔX and ΔY are used to solve for orthogonality errors, δ_N and δ_R.

First, the corrections, ΔX and ΔY, due to lack of orthogonality δ_N between the positive X and Y axes are given, in the following section, as

$$\tan\Delta X = \sin\delta_N \tan Y' \quad \text{(A-11)}$$

$$\tan\Delta Y = \frac{(1 - \cos\Delta X \cos\delta_N)\tan Y}{\tan^2 Y + \cos\delta_N \cos\Delta X} \quad \text{(A-12)}$$

for small δ_N, and $\tan\Delta Y < (\delta_N^2 + \delta_X^2)/2$.

Equations (A-11) and (A-12) reduce to:

$$\Delta X \approx \delta_N \tan Y' \quad \text{(A-13)}$$

$$\Delta Y \simeq 0 \quad \text{(A-14)}$$

See the description accompanying Figs. A-2 and A-3 for the explanation of symbols.

Second, the corrections, ΔX and ΔY, due to lack of orthogonality δ_R between the RF and Y axes are given from appendix section II-B as

$$\sin\Delta X = \frac{\sin\delta_R}{\cos Y} \quad \text{(A-15)}$$

$$\sin\Delta Y = \tan Y' (\cos\Delta Y - \cos\delta_R) \quad \text{(A-16)}$$

For small δ_R, these reduce to:

$$\Delta X \simeq \frac{\delta_R}{\cos Y'} \qquad \text{(A-17)}$$

$$\Delta Y \simeq 0 \qquad \text{(A-18a)}$$

where

$$\sin \Delta Y < \tan Y \cdot \delta_R^2$$

Since these corrections are very small, the total corrections to X and Y may be added and written as:

$$\Delta X_{total} \simeq \frac{\delta_N \sin Y' + \delta_R}{\cos Y'}$$

$$\Delta Y_{total} \simeq 0 \qquad \text{(A-18b)}$$

where

$$X \simeq X' - \Delta X$$

$$Y \simeq Y' \qquad \text{(A-18c)}$$

A. X and Y Axes Nonorthogonal

Figure A-2 is developed by first rotating X angle (from P_0 to M) about the antenna X axis, OP_2; then Y angle is rotated about the new Y axis. X angle below OP_1 is not shown. Thus OP_0 has been rotated to point N at the target in direction ON, about orthogonal axes. Secondly, consider the antenna Y axis OP_1 to be rotated so that it makes angle $(90 - \delta_N)^\circ$ with the antenna X axis OP_2. Now rotate X' angle from P_0 to P_0' about the antenna Y axis OQ. Thus OP_0 has been rotated to a point at the target in direction ON, about nonorthogonal axes.

The angle differences $\Delta X = X' - X$ and $\Delta Y = Y' - Y$ are the corrections to be subtracted from X' and Y' respectively to correct for this particular lack of orthogonality. Any Y axis error component about the X axis will be absorbed in the boresight error.

Consider the right spherical triangle $P_0'MN$ to obtain ΔX and ΔY.

$$\bar{\alpha} = (90 - \delta_N)^\circ, \quad \bar{\gamma} = 90^\circ$$

from spherical triangle relations:

$$\cos \bar{\alpha} = \tan \Delta X \cot Y'$$

Hence,

$$\sin \delta_N = \tan \Delta X \cot Y'$$

or

$$\tan \Delta X = \sin \delta_N \tan Y' \qquad \text{(A-19)}$$

Let

$$Y' = Y + \Delta Y,$$

Hence,

$$\tan (Y + \Delta Y) = \frac{\tan Y + \tan \Delta Y}{1 - \tan Y \tan \Delta Y}$$

by using Eq. (A-19)

$$\frac{\tan Y + \tan \Delta Y}{1 - \tan Y \tan \Delta Y} = \frac{\tan \Delta X}{\sin \delta_N} \qquad \text{(A-19a)}$$

Also, from the right triangle $P_0' MN$, spherical trigonometry gives

$$\sin \Delta X = \tan Y \tan \delta_N \qquad \text{(A-19b)}$$

substituting tan Y in Eq. (A-19a).

Hence,

$$\frac{\dfrac{\sin \Delta X}{\tan \delta_N} + \tan \Delta Y}{1 - \dfrac{\sin \Delta X \tan \Delta Y}{\tan \delta_N}} = \frac{\tan \Delta X}{\sin \delta_N}$$

or by cross multiplication:

$$\sin \Delta X \cos \delta_N + \tan \Delta Y \sin \delta_N = \tan \Delta X - \frac{\sin^2 \Delta X \tan \Delta Y}{\cos \Delta X \tan \delta_N}$$

and by rearranging tan ΔY terms:

$$\tan \Delta Y = \frac{\tan \Delta X - \sin \Delta X \cos \delta_N}{\sin \delta_N + \dfrac{\sin^2 \Delta X}{\cos \Delta X \tan \delta_N}}$$

Also, dividing by sin ΔX gives

$$\tan \Delta Y = \frac{\frac{1}{\cos \Delta X} - \cos \delta_N}{\frac{\tan \Delta X}{\tan \delta_N} + \frac{\sin \delta_N}{\sin \Delta X}}$$

substituting for tan δ_N and sin ΔX using Eq. (A-19b)

$$\tan \Delta Y = \frac{\frac{(1 - \cos \delta_N \cos \Delta X)}{\cos \Delta X}}{\frac{\tan \Delta X \tan Y}{\sin \Delta X} + \frac{\sin \delta_N}{\tan Y \tan \delta_N}}$$

Hence,

$$\tan \Delta Y = \frac{1 - \cos \delta_N \cdot \cos \Delta X}{\tan Y + \frac{\cos \delta_N \cos \Delta X}{\tan Y}} \qquad \text{(A-20)}$$

Substituting the Taylor series expansion:

$$\cos \delta_N \simeq 1 - \frac{\delta_N^2}{2}$$

$$\cos \Delta X \simeq 1 - \frac{\Delta X^2}{2}$$

and noting that the minimum value of the denominator in Eq. (A-20) is 2, the numerator becomes:

$$1 - \left(1 - \frac{\delta_N^2}{2}\right)\left(1 - \frac{\Delta X^2}{2}\right) \cong \frac{\delta_N^2}{2} + \frac{\delta_X^2}{2}$$

As $\tan \Delta Y \approx \Delta Y$ for ΔY as small as indicated above, and since $\delta_N \leqslant \Delta X$ for $Y \geqslant 45°$

$$\Delta Y \leqslant \delta_N^2$$

or

$$\Delta Y \simeq 0, \quad Y \geqslant 45° \qquad \text{(A-21)}$$

In all cases $\Delta Y < \frac{\delta_N^2 + \Delta X^2}{2}$

Thus Eq. (A-19) becomes

$$\Delta X \simeq \delta_N \cdot \tan Y' \qquad \text{(A-22)}$$

B. Y and RF Axis Nonorthogonal

Figure A-3 similarly illustrates the angular corrections required by an angle $(90 - \delta_R)°$ between the Y axis of the antenna (OS_1) and RF(OT_1) axis as shown (OT_0), instead of 90°. The RF axis error component about the Y axis will be absorbed by the boresight error.

First, rotate the orthogonal RF axis angle X from T_1 to T_1' about the antenna X axis OS_3. Then rotate angle Y from T_1' to T_1'' about the new Y axis (not shown), which is angle X below OS_1. Second, rotate OT_0 by angle X' to OT_0' about the X axis. Note that OT_1 moved to OT_2. Then rotate angle Y' from T_0' to T_1'' about the new Y axis OS_2. Note that T_2 moves to T_2' under this Y' rotation. Arc $S_2T_1''T_2' = 90°$ and is part of a great circle and is $\angle S_2\ OT_2' = 90°$. Arc S_2S_3 is also part of a great circle whose plane is $\perp$ to $T_0'O$. Arc $S_2T_1''T_2' \perp$ arc $T_2T_2'S_3$ at T_2'.

In Fig. A-3, $\Delta X = (X' - X)$, so ΔX must be subtracted algebraically from X' to obtain the true X. $\Delta Y = (Y' - Y)$, so ΔY must be algebraically subtracted from Y' to obtain the true Y. Spherical triangle $S_2S_3T_1''$ of Fig. A-3 provides solutions for ΔX and ΔY. Since

$$\cos (90 - \delta_R) = \cos 90 \cos (90 - Y) + \sin (90 - Y) \cos (90 - \Delta X) .$$

Hence,

$$\sin \delta_R = \cos Y \sin \Delta X$$

or

$$\sin \Delta X = \sin \delta_R / \cos Y \qquad \text{(A-23)}$$

Also, since

$$\cos (90 - Y) = \cos (90 - \delta_R) \cos 90 + \sin (90 - \delta_R) \sin 90 \cos (90 - Y')$$

then

$$\sin Y = \cos \delta_R \sin Y' \qquad \text{(A-24)}$$

Substituting

$$Y = Y' - \Delta Y,$$

Equation (A-24) gives:

$$\sin Y' \cos \Delta Y - \cos Y' \sin \Delta Y = \cos \delta_R \sin Y'$$

or

$$\sin \Delta Y = \frac{-\cos \delta_R \sin Y' + \sin Y' \cos \Delta Y}{\cos Y'}$$

or

$$\sin \Delta Y = \tan Y' (\cos \Delta Y - \cos \delta_R) \qquad \text{(A-25)}$$

Similarly by substituting $Y' = (Y + \Delta Y)$ into Eq. (A-24) gives

$$\sin Y = \cos \delta_R \sin Y \cos \Delta Y + \cos \delta_R \cos Y \sin \Delta Y$$

or

$$\sin \Delta Y = \frac{\sin Y - \cos \delta_R \sin Y \cos \Delta Y}{\cos \delta_R \cos Y}$$

or

$$\sin \Delta Y = \left(\frac{1}{\cos \delta_R} - \cos \Delta Y \right) \tan Y \qquad \text{(A-26)}$$

$$\text{Since for } 90° > \begin{pmatrix} Y \\ \text{and} \\ Y' \end{pmatrix} > 0, \begin{pmatrix} \tan Y \\ \text{and} \\ \tan Y' \end{pmatrix} > 0$$

and since

$$\left(\frac{1}{\cos \delta_R} - \cos \Delta Y \right) > 0 \text{ due to } \frac{1}{\cos \delta_R} > \cos \Delta Y,$$

$\sin \Delta Y > 0$ from Eq. (A-26), which makes $\cos \Delta Y > \cos \delta_R$

$$\left.\begin{array}{l} \cos \Delta Y > \cos \delta_R \\ \delta_R > \Delta Y \end{array}\right\} \qquad \text{(A-27)}$$

From Eq. (A-26):

$$\sin \Delta Y < \tan Y \left[1 + \frac{\delta_R^2}{2} - \left(1 - \frac{\Delta Y^2}{2} \right) \right]$$

From Eq. (A-27)

$$\sin \Delta Y < \tan Y (\delta_R^2) \qquad \text{(A-28)}$$

or

$$\Delta Y \simeq 0$$

Equation (A-23) then becomes Eq. (A–17):

$$\Delta X \simeq \frac{\delta_R}{\cos Y'} \qquad \text{(A-29)}$$

III. Partial Derivatives of *X* and *Y* Angles and Associated Error Terms

Errors in X and Y angles due to an error in a parameter P may be expressed by retaining only the linear term of a Taylor series expansion of the parameter so that

$$P = P_e + \Delta P$$

where P_e is the estimated value of P, and ΔP is the error in the estimate of P. Then the error in X (and similarly in Y) resulting from errors in estimating n parameters is,

$$\Delta X = \sum_{i=1}^{n} \left(\frac{\partial X}{\partial P} \right)_i \Delta P_i, \quad \Delta Y = \sum_{i=1}^{n} \left(\frac{\partial Y}{\partial P} \right)_i \Delta P_i$$

IV. Correction Due to Errors in Station Location

Errors in station latitude and longitude $\Delta\phi$ and $\Delta\lambda$ cause errors in X and Y angles as shown in Eqs. (A-30) and (A-31) below:

$$\Delta X = \frac{\partial X}{\partial \phi} \Delta\phi + \frac{\partial X}{\partial \lambda} \Delta\lambda \qquad \text{(A-30)}$$

$$\Delta Y = \frac{\partial Y}{\partial \phi} \Delta\phi + \frac{\partial X}{\partial \lambda} \Delta\lambda \qquad \text{(A-31)}$$

The partial derivatives are shown below. X and Y angles of a target can be related to the local hour angle t and declination δ of the target by

$$X = \sin^{-1}\left(\frac{-\cos\delta\sin t}{\cos Y}\right) \tag{A-32}$$

$$Y = \sin^{-1}(\sin\delta\cos\phi - \cos\delta\sin\phi\cos t) \tag{A-33}$$

Local hour angle t is a function of constants and of station longitude, so the partial derivatives with respect to t are equivalent to partial derivative with respect to λ.

Taking partial derivatives of Eqs. (A-32) and (A-33) with respect to ϕ and λ (or t) yields the four partial derivatives required by Eqs. (A-30) and (A-31).

The results are listed as:

$$\left(\frac{\partial Y}{\partial\lambda}\right)_\phi = \frac{\sin\phi\cos\delta\sin t}{\sqrt{1-(\sin\delta\cos\phi-\sin\phi\cos\delta\cos t)^2}} \tag{A-34}$$

$$\left(\frac{\partial X}{\partial\lambda}\right)_\phi = \frac{-\cos Y\cos\delta\cos t-\cos\delta\sin t\sin Y\left(\frac{\partial Y}{\partial\lambda}\right)}{\cos^2 Y\sqrt{1-\left(\frac{\cos\delta\sin t}{\cos Y}\right)^2}} \tag{A-35}$$

$$\left(\frac{\partial Y}{\partial\phi}\right)_\lambda = \frac{-\sin\delta\sin\phi-\cos\phi\cos\delta\cos t}{\sqrt{1-(\sin\delta\cos\phi-\sin\phi\cos\delta\cos t)^2}} \tag{A-36}$$

$$\left(\frac{\partial X}{\partial\phi}\right)_\lambda = \frac{-\cos\delta\sin t\sin Y\left(\frac{\partial Y}{\partial\phi}\right)}{\cos^2 Y\sqrt{1-\left(\frac{\cos\delta\sin t}{\cos Y}\right)^2}} \tag{A-37}$$

V. Errors Due to Structural Deflection

As described earlier, X and Y deflection errors are assumed to be maximum at a near-horizon-reference $\bar{\phi}$ and minimum at an elevation angle $(h-\bar{\phi}) = 90°$, where h is the antenna elevation angle. Deflection errors in an elevation plane are transformed into X and Y errors by using partial derivatives with respect to h.

The deflection errors in X and Y angles are

$$\Delta X = C_1\cos(h-C_2)\left(\frac{\partial X}{\partial h}\right)_\psi \tag{A-38}$$

$$\Delta Y = C_4\cos(h-C_5)\left(\frac{\partial Y}{\partial h}\right)_\psi \tag{A-39}$$

The partial derivatives are derived below utilizing the X-Y to azimuth (ψ), elevation (h) transformations. The partials required by Eqs. (A-38) and (A-39) are given in Eqs. (A-47) and (A-48), where the derivation is made as follows:

$$\sin h = \cos Y\cos X \tag{A-40}$$

$$\cos h\sin\psi = \cos Y\sin X \tag{A-41}$$

$$\sin Y = \cos h\cos\psi \tag{A-42}$$

Partial derivative with respect to h of (A-42) gives:

$$\cos Y\left(\frac{\partial Y}{\partial h}\right)_\psi = -\sin h\cos\psi$$

And substitution of $\cos\psi$ from (A-42) delivers

$$\left(\frac{\partial Y}{\partial h}\right)_\psi = \frac{-\sin h}{\cos Y}\cdot\frac{\sin Y}{\cos h} = -\tan h\tan Y \tag{A-43}$$

Division of (A-41) by (A-40) provides,

$$\frac{\cos Y\sin X}{\cos Y\cos X} = \frac{\cos h\sin\psi}{\sin h}$$

or

$$\tan X = \cot h\sin\psi \tag{A-44}$$

Differentiating (A-44) with respect to h,

$$\sec^2 X\left(\frac{\partial X}{\partial h}\right)_\psi = -\csc^2 h\sin\psi \tag{A-45}$$

Use of Eqs. (A-40) and (A-41) simplifies (A-45) to

$$\left(\frac{\partial X}{\partial h}\right)_\psi = \frac{-\cos Y\sin X\cos^2 X}{\cos h\sin^2 h} = \frac{-\cos Y\sin X}{\cos h\cos^2 Y}$$

$$= \frac{-\sin X}{\cos h\cos Y} \tag{A-46}$$

Finally from (A-43) and (A-46)

$$\left(\frac{\partial X}{\partial h}\right)_{\psi=const} = -\frac{\sin X}{\cos h\cos Y} \tag{A-47}$$

$$\left(\frac{\partial Y}{\partial h}\right)_{\psi=const} = -\tan h \tan Y \qquad \text{(A-48)}$$

VI. Boresight Shift with Polarization Rotation

A common characteristic of the circularly polarized monopulse tracking antenna is that a boresight shift occurs as the receive signal polarization vector is rotated with respect to the receiving antenna feed. The greater the axial ratio of the received polarized signal, the greater the magnitude of the boresight shift. The boresight shift varies in a systematic manner with the rotation of the polarization vector of the incident electromagnetic waves. In general, a relative rotation of the polarization vectors of 180 degrees will result in the boresight of the monopulse antenna traversing an ellipse (in the orthogonal angular coordinates of the antenna) centered on the nominal boresight. In general, the orientation of the ellipse relative to the orthogonal angular coordinate of the antenna is arbitrary.

In general, all aircraft tracks are commonly performed with a linear (vertical) polarized transmit signal and an elliptically polarized receiving antenna. The motion of the X-Y mount antenna is such that, throughout tracking, the orientation of the tracking feed is rotated about the line-of-sight axis. For a typical track, this can result in a significant shifting of the system boresight throughout the track. Thus it is necessary that the boresight shift with polarization rotation error term be included in the reduction of tracks in order to determine the proper values for the other error model terms.

Referencing the feed system space angles, the Y and cross-Y components of the boresight shift are given by the generalized parametric equations of an ellipse:

$$ERROR_{CY} = A_9 \sin 2\theta \qquad \text{(A-49)}$$

$$\begin{aligned} ERROR_Y &= M \sin(2\theta + N) \\ &= M(\sin 2\theta \cos N + \cos 2\theta \sin N) \\ &= A_{10} \sin 2\theta + A_{11} \cos 2\theta \end{aligned} \qquad \text{(A-50)}$$

where

$A_{10} = M \cos N$,

$A_{11} = M \sin N$,

θ is the angle between a reference line on the feed which is vertical (when the XY mount faces the east or south horizon depending on the antenna design and a constantly vertical line, representing the vertical transmit polarization).

N is the angle between the radial lines which pass through the tangent points of the ellipse and the lines $ERROR_{CY} = A_9$ and $ERROR_Y = M$, respectively (refer to Fig. A-4).

$$\theta = \tan^{-1}\left(\frac{\cos X \sin Y}{\sin X}\right)$$

and since the regression equations are solved in X angle (antenna shaft angle) rather than cross-Y (space angle), Eqs. (A-49) and (A-50) become:

$$ERROR_X = \frac{ERROR_{CY}}{\cos Y} = \frac{A_9 \sin 2\theta}{\cos Y} \qquad \text{(A-51)}$$

$$ERROR_Y = A_{10} \sin 2\theta + A_{11} \cos 2\theta \qquad \text{(A-52)}$$

Equations (A-51) and (A-52) were incorporated into the total system angular error model for reduction of the system test data. Note that after regression estimates of A_9, A_{10}, and A_{11} are obtained, the maximum boresight shift with polarization of the antenna can be determined.

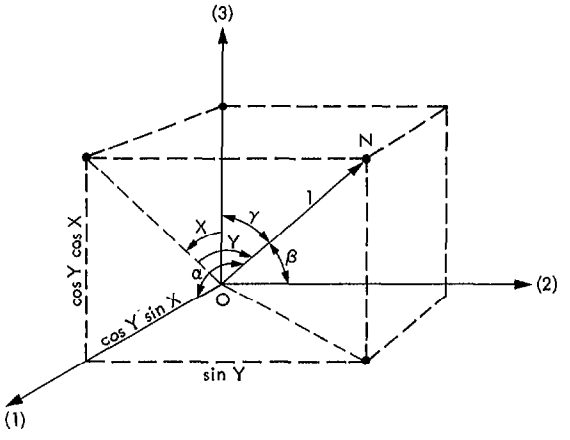

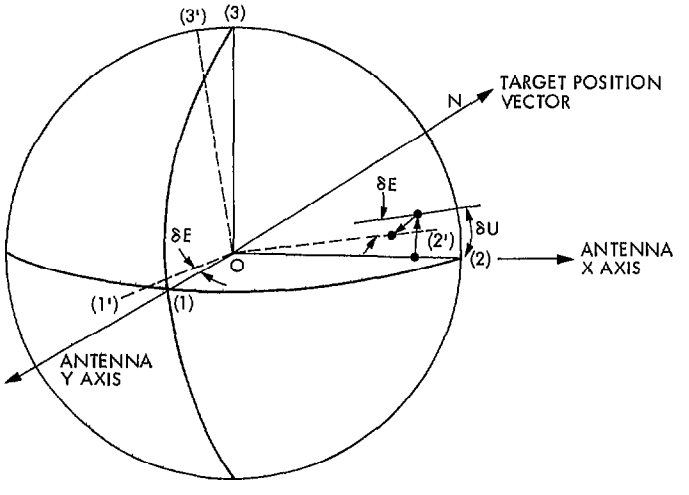

Fig. A-1. *Angle error derivations*

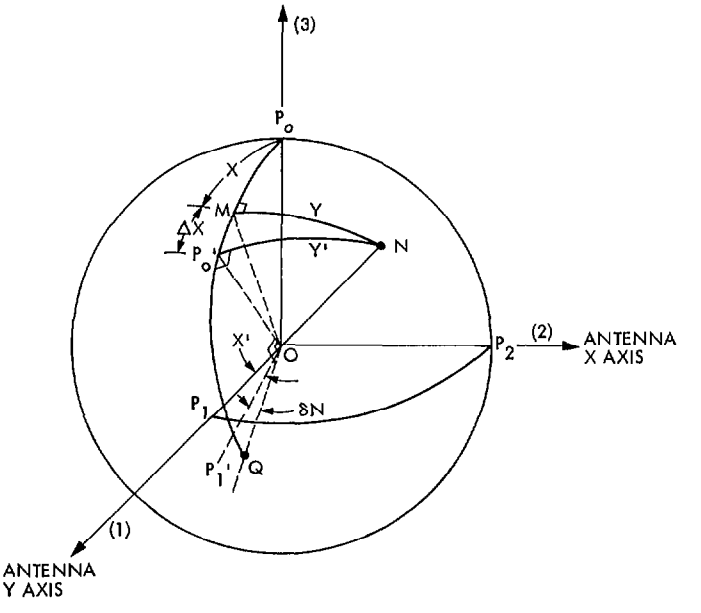

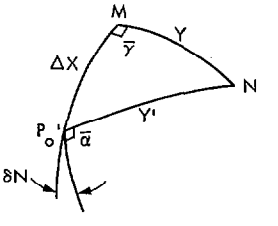

Fig. A-2. Orthogonality error derivations (1)

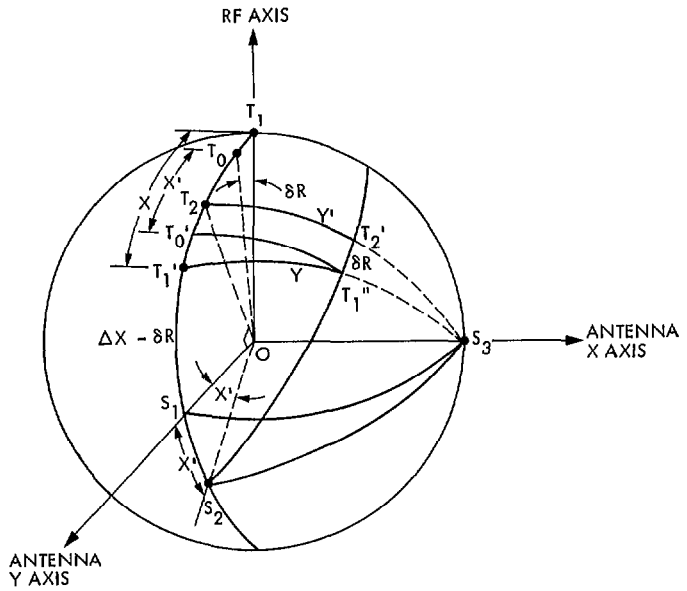

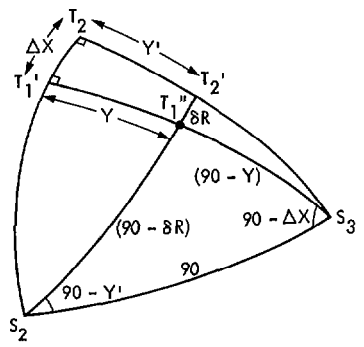

Fig. A-3. Orthogonality error derivations (2)

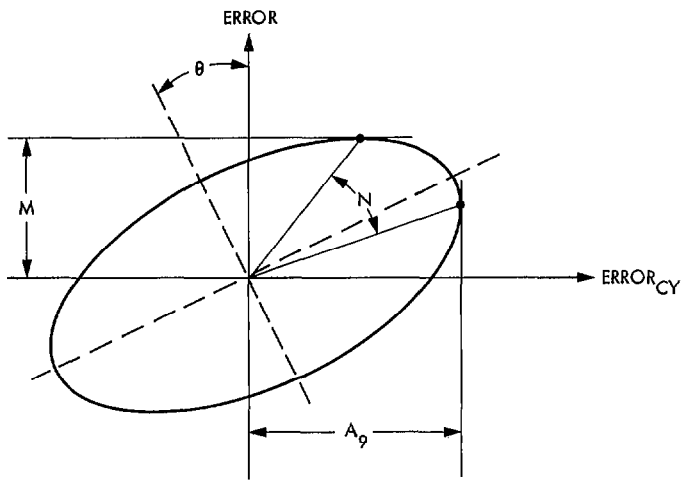

Fig. A-4. Geometrical relationships for boresight shift with polarization model